

# STATISTICAL MODELS FOR CLOSE BINARIES

J.L. Halbwachs  
Observatoire de Strasbourg, France

**ABSTRACT.** Statistical models for binaries as a whole were selected; then statistical properties of close binaries -the proportions of spectroscopic and eclipsing binaries and the distributions of the K velocities and of the depths of eclipse- were computed for each model.

## 1. INTRODUCTION

The statistical models describe the distributions of binaries according to their physical parameters. These parameters are: -the semimajor axis of the orbit, "a" ; -the mass ratio of the system, here defined as the ratio  $q = M_2/M_1 < 1$ ; -the inclination of the orbit, "i", and -the eccentricity, "e", which may be neglected in a first approach. The models can be tested on observable features, as will be shown later.

## 2. SELECTION OF THE MODELS

In order to evaluate the observational consequences of the models, some typical distributions were assumed for each of the above mentioned parameters. 3 possible distributions for the logarithm of "a" are illustrated in Figure 1 and 4 distributions of "q" in Figure 2. The inclinations

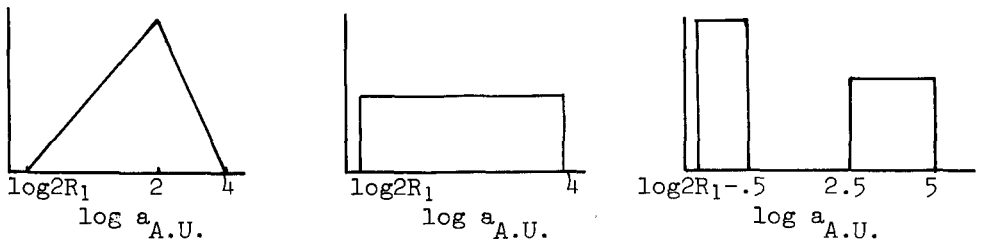


Figure 1. Selected distributions of  $\log a$ ;  $R_1$  is the radius of the primary component of the system.

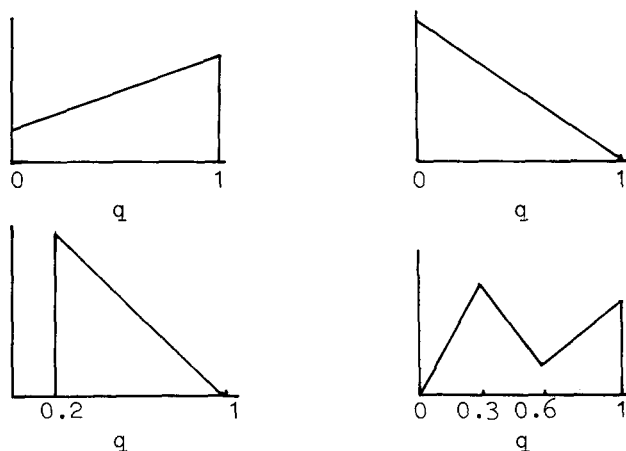


Figure 2. Selected distributions of  $q$ .

are assumed to be randomly distributed.

To derive statistical characteristics of the spectroscopic and of the eclipsing binaries, all the 12 combinations of the selected distributions of "a" and "q" were considered.

### 3. APPLICATIONS TO SPECTROSCOPIC BINARIES

#### 3.1. Distribution of the semi-amplitudes of radial velocities

The distribution of the semi-amplitudes of the radial velocities of the primary components, "K", was computed by sampling experiments for binaries with solar-type primary components. It was found that when the distribution of  $\log a$  is unimodal, the resulting distribution of K reflects  $f(\log a)$  rather than  $f(q)$ . Figure 3 gives the distributions of K obtained for the constant and for the triangular distributions of  $\log a$ . The distributions of "q" give results lying inside the hatched areas.

When the distribution of  $\log a$  is bimodal, the distribution of K may show a gap depending on the distribution of  $q$ . When the distribution of  $q$  is decreasing from  $q = 0$ , the gap disappears, but the shape of the curve strongly differs from the unimodal cases (cf Figure 4).

When binaries have eccentric orbits, the value of K increases but the curve of radial velocity is distorted and exhibits a narrow peak. Therefore the increase of K can be compensated by the low probability of measuring a velocity near the maximum and it is consequently very convenient to substitute K by half of the range in radial velocity observed if 5 to 10 measures per star are available. As an example, Figure 5 gives the distributions of K obtained from 5 measures per star for 2 synthetic samples which differ only in eccentricities: in the first sample,

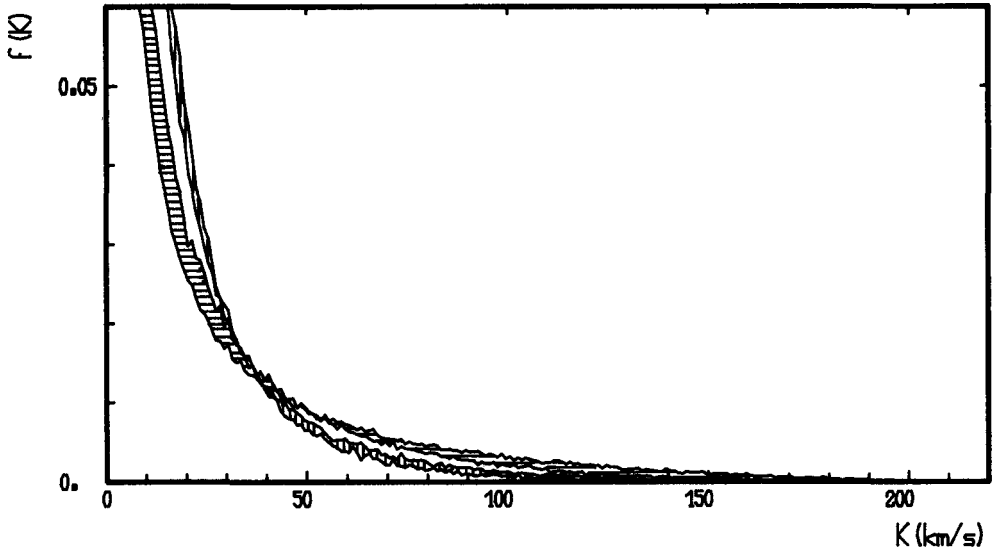


Figure 3. Distributions of  $K$  according to the assumed  $f(\log a)$ . Graphs are normalized for systems with  $K > 15$  km/sec . The horizontal hachures denote the constant  $f(\log a)$  and the vertical hachures denote the triangular  $f(\log a)$ .

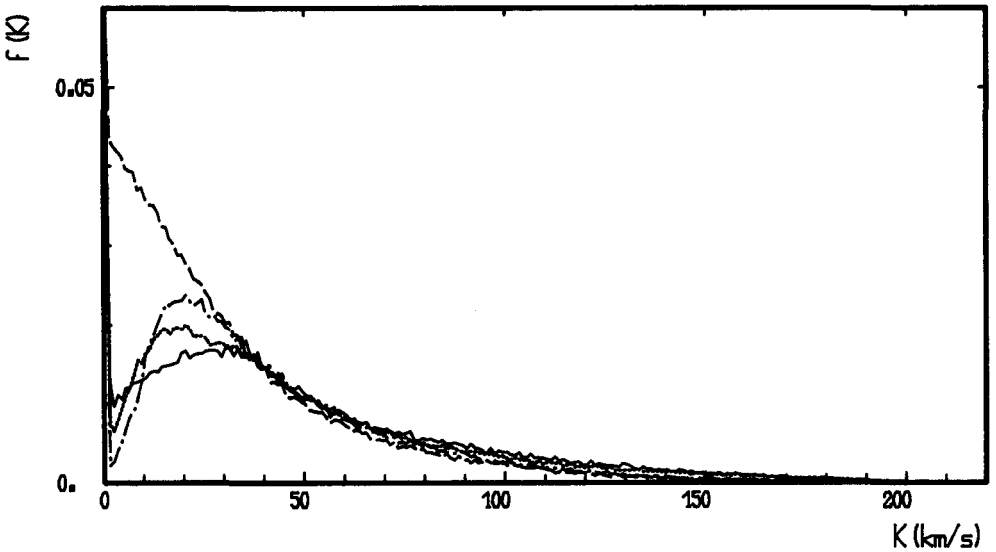


Figure 4. Distributions of  $K$  in the case of a bimodal distribution of  $\log a$ . The distributions of  $q$  are identified as follow : Unbroken line: increasing distribution. Dashed line: decreasing distribution. Dashes and dots : distribution decreasing from  $q=0.2$ . Dotted line: bimodal distribution. Graphs are normalized as in Figure 3.

binaries have all non-eccentric orbits, while the orbits in the second sample have all the eccentricity 0.5. It is easy to see that the agreement between the two resulting distributions of  $K$  is very good.

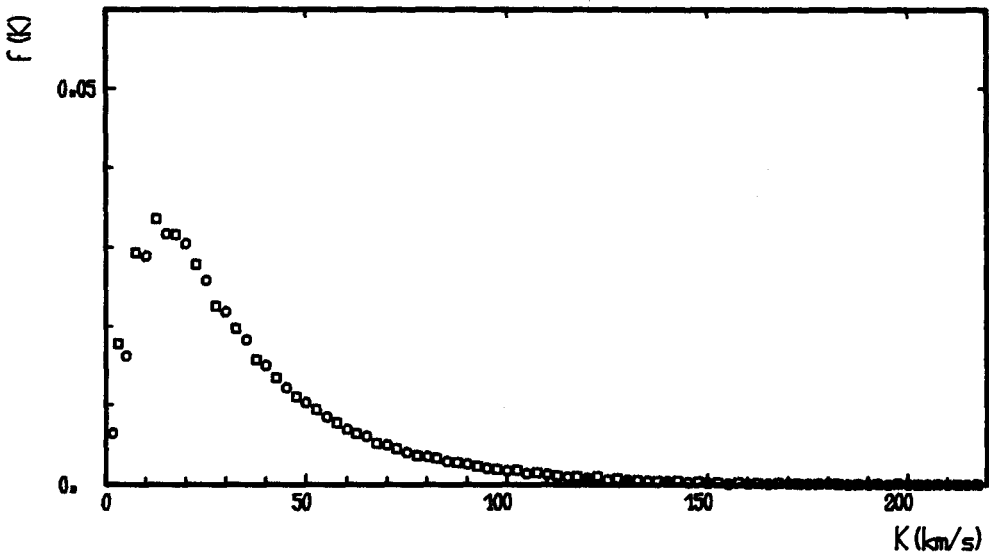


Figure 5. Distributions of  $K$  observed in 5 measures per star in the case of  $f(\log a)$  bimodal and  $f(q)$  decreasing from 0.2 for two samples with different eccentricities: the circles denote a sample with  $e=0$  and the squares denote a sample with  $e=0.5$ . The distributions are normalized as in Figure 3.

Thus it is possible to consider for statistical purposes binaries with unknown orbit as long as at least 5 measures of radial velocity are available for each star.

### 3.2. Proportion of spectroscopic binaries

In order to evaluate the proportion of detectable spectroscopic binaries, the binaries with  $K$  higher than 15 km/sec were considered. As shown in Figure 6, these proportions lie between 6 and 43 per cent and depend mainly on the distribution of  $\log a$ .

## 4. APPLICATION TO ECLIPSING BINARIES

### 4.1. Distribution of the depths of primary eclipses

The depths of primary eclipses were computed according to the "spherical model"; this model neglects all proximity effects occurring in close binaries (i.e. stars are considered to be spheres), but includes the limb darkening. Primary components were assumed to be dwarfs with spectral

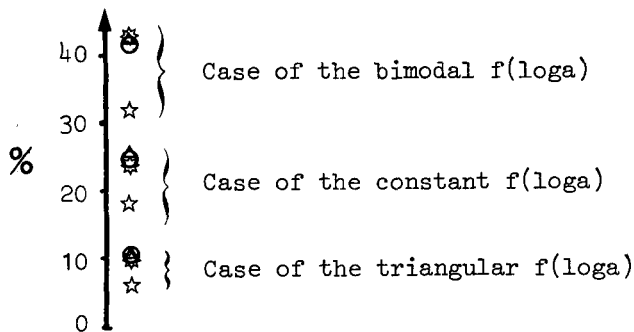


Figure 6. Proportions of binaries for which  $K > 15$  km/sec. The distributions of  $q$  are identified as follow :  $\Delta$  : increasing distribution.  $\star$  : decreasing distribution.  $\odot$  : distribution decreasing from  $q=0.2$ .  $\circ$  : bimodal distribution.

types lying between F and M. As a consequence of the random distribution of the inclinations, the distribution of the depths of eclipse depends only on the distribution of the mass ratios. The distributions normalized on the systems with eclipse deeper than 0.4 are given in Figure 7. Notice that the distribution of mass ratios decreasing from  $q=0.2$  produces a gap near  $\Delta m = 0.13$ , which is the upper limit for the eclipses of systems with  $q=0.2$ .

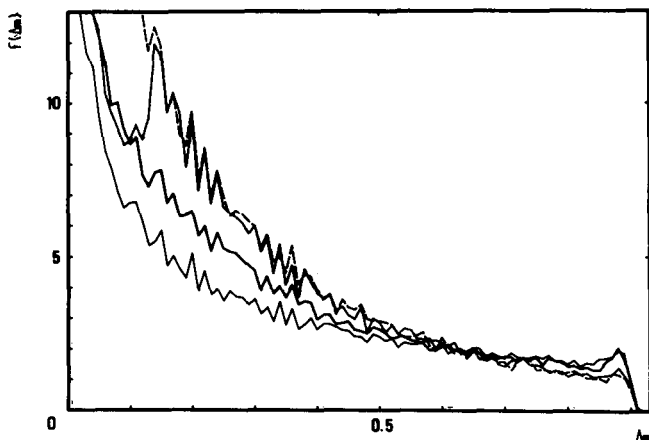


Figure 7. Distributions of the depths of primary eclipse; the distributions of  $q$  are identified as in Figure 4.

#### 4.2. Proportion of eclipsing binaries

The proportion of binaries that may undergo an eclipse can be derived from :

$$P(\Delta m > 0) = R_1 < 1/a > < 1+q^\alpha > \tag{1}$$

$\alpha$  being the coefficient of the mass-radius relation :

$$R_1/R_0 = (M_1/M_0)^\alpha \tag{2}$$

and for dwarfs,  $\alpha = 0.75$  . Due to the difficulties of detectability, the proportions of binaries which present eclipse deeper than 0.4 were also computed. Results are shown in Figure 8. As in the case of spectroscopic binaries, the distribution of semimajor axes predominates in the results.

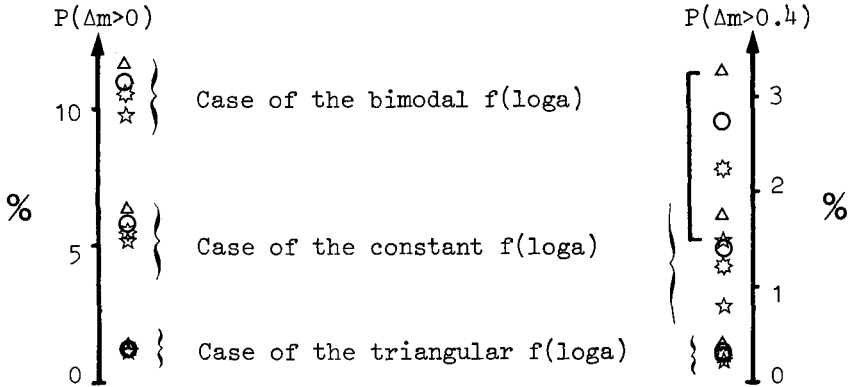


Figure 8. Proportions of binaries with eclipse deeper than 0 (left) or than 0.4 (right). The distributions of  $q$  are identified as in Figure 6.

The use of the spherical model being inadequate for very close systems, the proportions of binaries that undergo eclipse were computed again by assuming that all binaries closer than 5 times the primary radius are eclipsing. In this case, the proportions increase by 1.4 when the distribution of  $\log a$  is triangular and by 1.7 in the two other cases.

Additional information on the models, the computation of the observable characteristics and the practical range of application of the results is provided in Halbwachs (1981 a,b).

It is a pleasure to thank Prof. C. Jaschek for his support and guidance of this project.

REFERENCES

Halbwachs, J.L.: 1981a, *Astron. Astrophys.* in press.  
 Halbwachs, J.L.: 1981b, "modèles statistiques pour l'étude des binaires serrées", thèse de troisième cycle, Observatoire de Strasbourg.